www.dergipark.gov.tr
ISSN:2148-3736
El-Cezerî Fen ve Mühendislik Dergisi
Cilt: 7, No: 2, 2020 (487-502)

El-Cezerî Journal of Science and Engineering
Vol: 7, No: 2, 2020 (487-502)
DOI :10.31202/ecjse.660136

ECJSE

Research Paper / Makale

Rotor Spacing and Blade Number Effect on the Thrust, Torque, and Power of a Coaxial Rotor

İbrahim GÖV

Aircraft and Aerospace Engineering Department, Gaziantep University, Gaziantep, Turkey
igov@gantep.edu.tr

Received/Geliş: 16.12.2019 **Accepted/Kabul:** 27.02.2020

Abstract: In this study, rotors space and number of the blade are examined in terms of the torque, power and thrust concept. Three-dimensional flow analysis was performed by using SolidWorks flow simulation. In aircraft propeller design, thrust, torque and power concept has a great deal of importance. The rotor can be defined as a propulsion system, which provides the thrust with a propeller. The pressure difference produces due to the velocity difference between the lower and upper surfaces of the airfoil. The thrust is obtained with this pressure difference. The rotor blades produce drag and thrust thanks to rotating airfoils. The number of the blade affects the amount of thrust directly. If the blade number of rotor increases, the produced thrust, torque by the rotor and the needed power to drive rotor will also increase. In this study, the effect of blade number (2, 3 and 4 blades) and distance between rotors (0.05*D, 0.1*D, 0.25*D, 0.5*D, 0.75*D, 1*D) on the thrust, torque and power are investigated.

Keywords: Rotor, CFD, Power, Thrust, Torque

Rotor Mesafesinin ve Kanat Sayısının bir Koaksiyel Rotorun İtkisine, Torkuna ve Gücüne Etkisi

Öz: Bu çalışmada rotor boşluğu ve kanat sayısı tork, güç ve itki kavramı açısından incelenmiştir. SolidWorks akış simülasyonu kullanılarak üç boyutlu akış analizi yapıldı. Uçak pervanesi tasarımında, itme, tork ve güç konseptinin önemi büyüktür. Rotor, pervane ile itki sağlayan tahrik sistemi olarak tanımlanabilir. Basınç farkı, kanat profilinin alt ve üst yüzeyleri arasındaki hız farkı nedeniyle oluşur. İtme kuvveti bu basınç farkı ile elde edilir. Dönen kanat profilleri sayesinde rotor kanatları sürükleme ve itme kuvveti üretir. Kanat sayısı doğrudan itme miktarını etkiler. Rotorun kanat sayısı arttıkça, rotor tarafından üretilen itki, tork ve rotoru çalıştırmak için gereken güç de artacaktır. Bu çalışmada kanat sayısının (2, 3 ve 4 kanat) ve rotorlar arasındaki mesafenin (0,05 * D, 0,1 * D, 0,25 * D, 0,5 * D, 0,75 * D, 1 * D) itkiye, torka ve güce etkisi incelenmiştir.

Anahtar kelimeler: rotor, HAD, güç, itki, tork

1. Introduction

A rotor is a type of fan that transmits power by converting rotational motion into thrust. A pressure difference is produced between the forward and rear surfaces of the airfoil-shaped blade, and a fluid (such as air or water) is accelerated behind the blade. Rotor dynamics, like those of aircraft wings, can be modeled by either or both Bernoulli's principle and Newton's third law [1]. Rotors are the most critical parts for the propulsion systems. In the literature, nearly all studies are focused on marine propellers. There are few studies that exist about aero propellers. Noh et al. [2] investigated

How to cite this article
Gör, İ., "*Rotor Spacing and Blade Number Effect on the Thrust, Torque and Power of a Coaxial Rotor",* El-Cezerî Journal of Science and Engineering, 2020, 7(2); 487-502.

Bu makaleye atıf yapmak için
Gör, İ., *"Rotor Mesafesinin ve Kanat Sayısının bir Koaksiyel Rotorun İtkisine, Torkuna ve Gücüne Etkisi",* El-Cezerî Fen ve Mühendislik Dergisi 2020, 7(2); 487-502.

different angles of attack values (25°, 35°, and 45°) effect on the airfoil and flat shape louvers. The symmetrical 4-digit NACA airfoil shape was used as louvers and it had 10 mm thickness. Solid Works Flow Simulation tool was used for CFD analysis. The results show that pressure drop is more widespread in flat louvers as compared to airfoil louvers. Hong and Dong [3] was presented a process for numerical analysis of the radial circulation distribution of the rotor blade. This process is based on the results of numerical simulation of the velocity field around rotor blades and in the wake. A method to estimate full-scale rotor torque and thrust consisting of low-frequency and high-frequency components in waves by a free-running model ship test were proposed by Ueno and Tsukada [4]. Driss et. al. [5] applied an experimental validation and numerical simulation to study the turbulent flow around a small incurved Savonius wind rotor. For the analysis, the Solid Works flow simulation tool was used. Navier-Stokes equations and standard k-ε turbulence model were used. These equations were solved by a finite volume discretization method. The effect of the ducted fan, which is located inside the ground effect region, is investigated experimentally according to the helicopter hovering concept by Doğru et. al. [6]. For this investigation, the thrust of the ducted fan is measured using two different experimental methods, which are static pressure measurement system and spring method to calculate the thrust. Lei et. Al. [7] studied on performance of a coaxial rotor. They used thrust and power consumption as performance parameters of the system and rotor spacing and wind speed as design parameters. Göv [8] investigated thrust, torque and power concepts according to different blade numbers (2, 3 and 4 blades). Yoon et. al. [9] investigated the effects of torque balancing on the performance of coaxial-rotor systems. Han et. al. [10] developed an efficient hybrid inverse/optimization design method that combines inverse design and direct optimization within a surrogate-based optimization (SBO) framework for rigid coaxial rotor airfoils considering reverse flow. Kavuran et. al. [11] developed an experimental test platform of a low-cost coaxial rotor for implementation of Model Reference Adaptive Controller (MRAC) with Fractional Order Adjustment Rules by using MATLAB/Simulink. Shukla and Komerath [12] investigated the interactions between wakes of two side-by-side rotors as a function of the distance between the rotors and their Re at from instantaneous as well as mean flow field perspective. Feil et. al. [13] developed a comprehensive analysis model of a laboratory-scale torque-balanced rotor designed for high-advance-ratio forward flight to investigate the aeromechanics of coaxial counter-rotating lift-offset rotor systems. Gül and Kolip [14] studied to increase the wing performance by reducing the reverse resistance in the convex blade of the Savonius wind turbine, which is a vertical axis wind turbine. Chen at. al. [15] presented a mechanical configuration of an independent pitch control system (IPCS) for a coaxial dual-rotor compound helicopter (CDCH), which is mainly constituted by parallel mechanism, spatial orientation, lower rotor, and upper rotor. Jiang et. al. [16] adopted Multiblock grids and Multiple Frame of Reference model to predict the complex viscous flow of multirotor, which transforms the time-dependent formulation into a steady-state approximation. The predictive capability of the new configuration as well as the SUAV was very high and validated by the experimental results. Yuan et. al. [17] proposed a coaxial compound configuration as a concept for future high-performance rotorcraft. Ferguson and Thomson [18] investigated the compounding of the conventional helicopter and how the addition of thrust and wing compounding influences the performance of this aircraft class. Santos-Medina et. al. [19] discussed the design and modeling of a spherical flying robot to control its hovering and omnidirectional mobility by controlling the air mass differential pressure between two asynchronous coaxial rotors that are aligned collinearly. Kim et. al. [20] investigated the aerodynamics and acoustics of a generic coaxial helicopter with a stiff main rotor system and a tail-mounted propulsor using Brown's Vorticity Transport Model. Enconniere et. al. [21] presented the development and application of a multidisciplinary methodology for the preliminary design assessment of compound coaxial rotorcraft with a counter-rotating rotor system and a rear-mounted propeller. Enconniere et. al. [22] presented the performance analysis of a coaxial counter-rotating rotor configuration with a pusher propeller to quantify the benefits of compound rotorcraft. Lyu and Xu [23] established a comprehensive

calculation model of a counter-rotating coaxial-rotor propeller-augmented compound helicopter based on the free-wake method to investigate its interactional aerodynamic characteristics.

After the literature review, it is seen that many studies are focused on marine propellers. There are few studies that exist about aero propellers. Also, the effect of the rotor distance and blade number on the performance of the coaxial rotor is not investigated in any study.

There are three theories used in the design of propellers. They are blade element, momentum, and vortex theory. Most of today's propellers are designed using blade element theory.

Induced velocity (eq. 1) and power (eq. 2) equations for coaxial rotors are given below:

$$(v_i)_e = \sqrt{\frac{(2T)}{2\rho A}} \tag{1}$$

$$(P_i)_{tot} = 2T(v_i)_e = \frac{(2T)^{3/2}}{\sqrt{2\rho A}} \tag{2}$$

If each rotor taken as separately the induced power (eq. 3) for each rotor is Tv_i and the sum of two is:

$$P_i = 2 \times \frac{T^{3/2}}{\sqrt{2\rho A}} \tag{3}$$

Calculating the interference-induced power factor (eq. 4):

$$K_{int} = \frac{(P_i)_{tot}}{P_i} = \frac{(2T)^{3/2}}{\sqrt{2\rho A}} \Big/ \frac{2T^{3/2}}{\sqrt{2\rho A}} = \sqrt{2} \tag{4}$$

Coaxial rotor increase of 41% in the induced power [7].

2. CFD Analysis

In this study, a numerical calculation method with the SolidWorks flow simulation tool is used for cases. A standard rotor is used in numerical calculations. In the numerical study, the external flow type is used (Figure 1). In addition, "exclude cavities without flow conditions" and "exclude internal space" are selected since the present study is not interested in cavities or spaces.

NACA 0012 airfoil is used to obtain the rotor as shown in Figure 2. In the numerical study 2 blades (in Figure 3), 3 and 4 blades (in Figure 4) rotors are used. 660 mm Rotor diameter is used for all rotors. Different rotor distances are investigated according to D which is rotor diameter as 0,05D, 0,1D, 0,25D, 0,5D, 0,7D, and 1D. Optimum rotor distance was obtained according to numerical results.

Air is defined as the fluid domain for the environment of the system as shown in Figure 5. Also, the Rotational domain is created as shown in Figure 6.

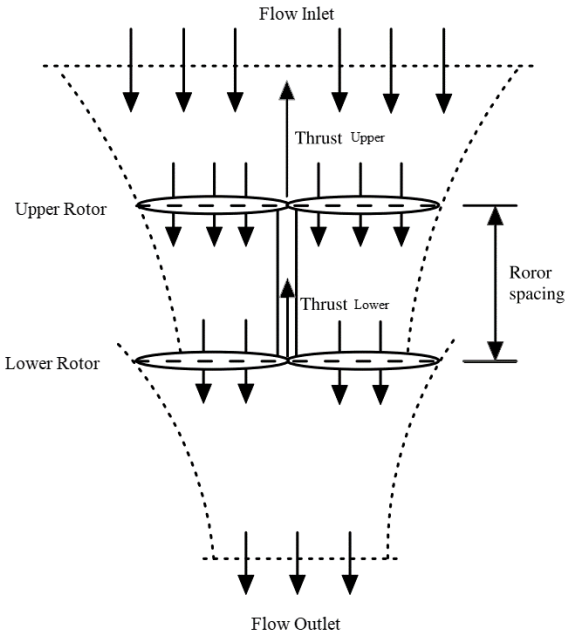

Figure 1. Coaxial rotor Flow Representation [7]

Figure 2. Blade airfoil [24]

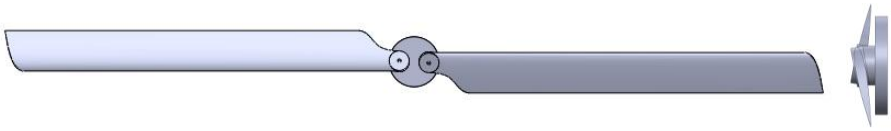

Figure 3. Front and side view of 2 blades rotor

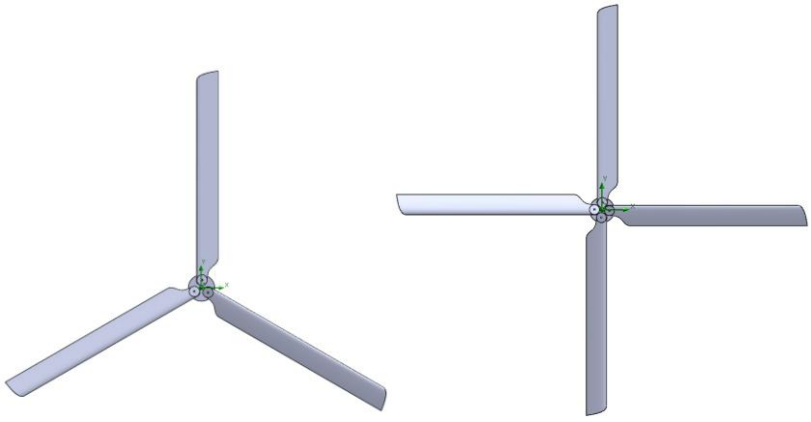

Figure 4. Front view of 3 blades and 4 blades rotors

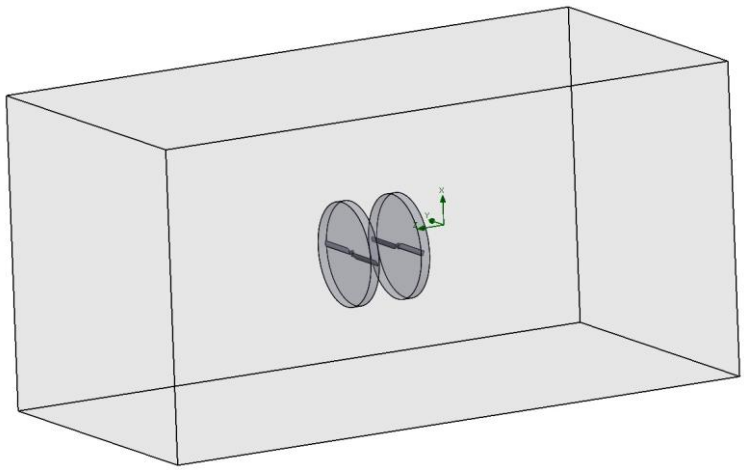

Figure 5. Simulation domain

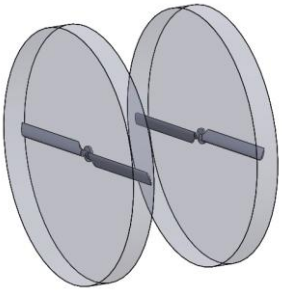

Figure 6. Rotational domain

Initial conditions are defined as: there is no velocity in any direction because there is no crosswind. Temperature is assumed to be room temperature (20° C) on the atmospheric pressure. This numerical study was performed at the 2500 RPM (261.71 rad/s).

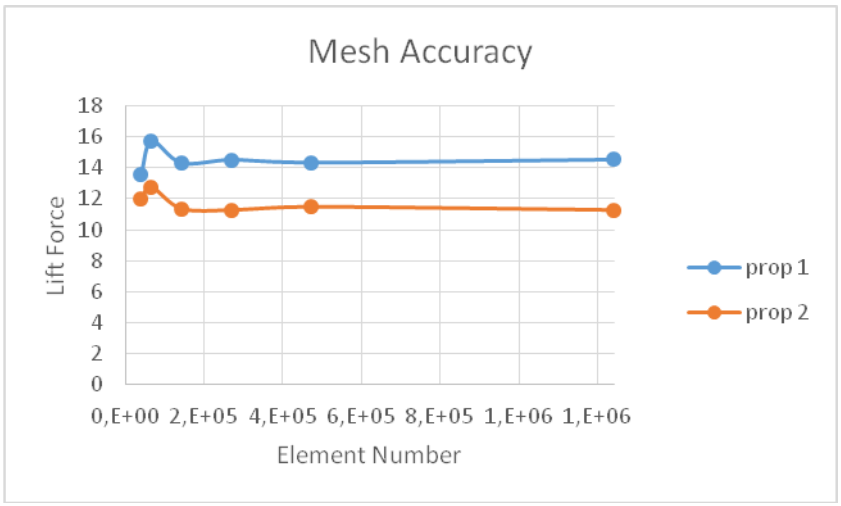

Figure 7. Mesh accuracy

The rotational region is covered with the environmental pressure to simulate the real conditions after the boundary conditions are defined. The element number effect is researched and the result is

given in Figure 7. As a result of this research, approximately 470000 element number is used in the analyses.

2. Results and Discussion

In this study, rotor thrust and torque values are calculated at different blade numbers and different rotor spacing values by using the SolidWorks flow simulation analysis program. Also, pressure distribution (in Figure 8) and velocity distribution (in Figure 9) are calculated for 0.05*D (33mm) rotor spacing. Flow distribution, tip flow distribution and flow lines are given in figures 10, 11 and 12 respectively for 0.05*D (33mm) rotor spacing.

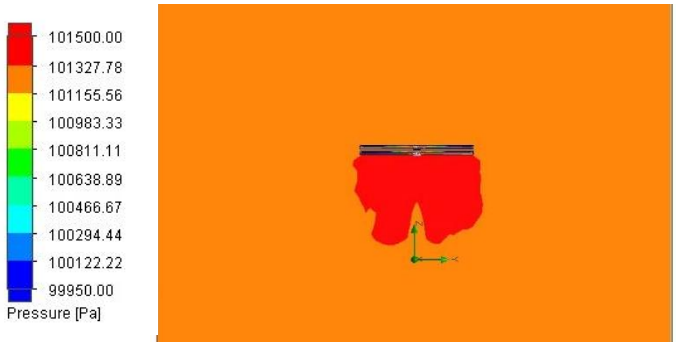

Figure 8. Pressure distribution of coaxial rotor at 0.05*D rotor spacing

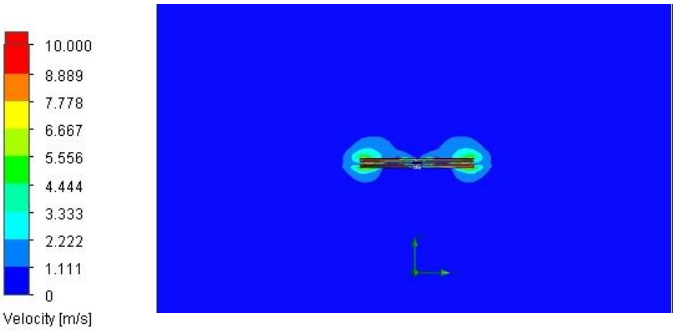

Figure 9. Velocity distribution of coaxial rotor at 0.05*D rotor spacing

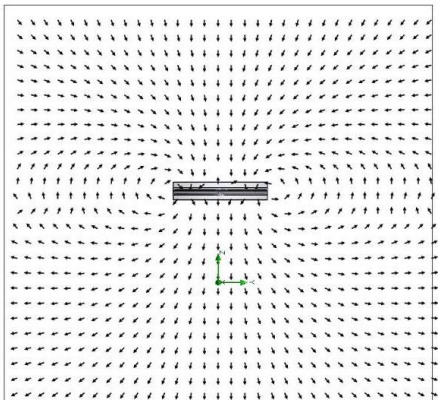

Figure 10. Flow distribution of coaxial rotor at 0.05*D rotor spacing

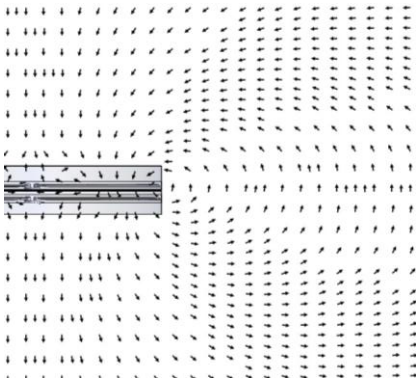

Figure 11. Tip flow distribution of coaxial rotor at 0.05*D rotor spacing

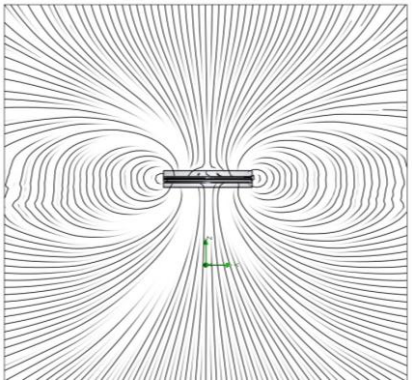

Figure 12. Flow lines of the coaxial rotor at 0.05*D rotor spacing

Pressure distribution (in Figure 13) and velocity distribution (in Figure 14) are calculated for 0.5*D (330mm) rotor spacing. Flow distribution, tip flow distribution and flow lines are given in figures 15, 16 and 17 respectively for 0.5*D (330mm) rotor spacing.

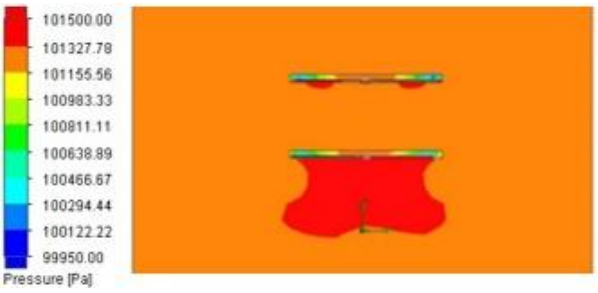

Figure 13. Pressure distribution of coaxial rotor at 0.5*D rotor spacing

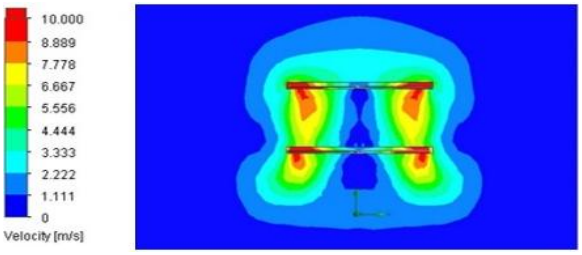

Figure 14. Velocity distribution of coaxial rotor at 0.5*D rotor spacing

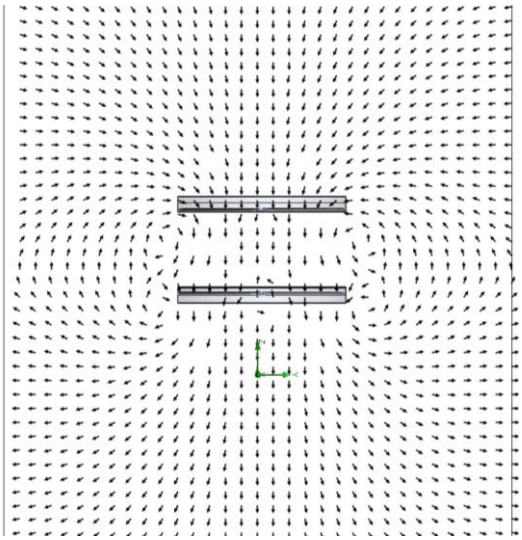

Figure 15. Flow distribution of coaxial rotor at 0.5*D rotor spacing

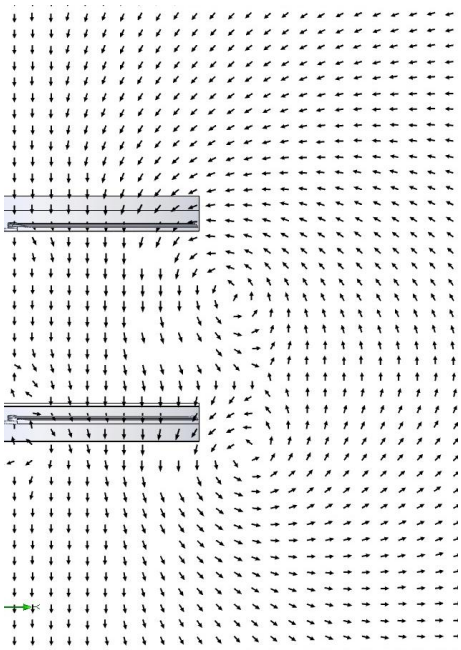

Figure 16. Tip flow distribution of coaxial rotor at 0.5*D rotor spacing

Thrust and torque values are calculated from the analysis program for the 2 blades single rotor as shown in Table 1.

Table 1. Results of 2 blades single rotor

2 Blades	Averaged Value
Thrust (N)	10,3
Torque (N*m)	0,77
Power (watt)	201,75
Thrust/Power	0,051

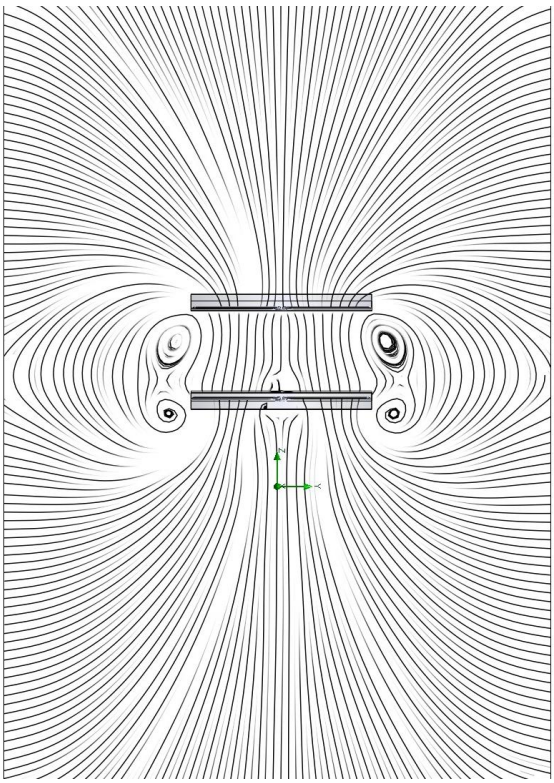

Figure 17. Flow lines of the coaxial rotor at 0.5*D rotor spacing

Thrust and torque value are calculated from the analysis program for the 3 blades single rotor as shown in Table 2.

Table 2. Results of 3 blades single rotor

3 Blades	Averaged Value
Thrust (N)	14,55
Torque (N*m)	0,99
Power (watt)	259,39
Thrust/Power	0,056

Thrust and torque value are calculated from the analysis program for the 4 blades single rotor as shown in Table 3.

Table 3. Results of 4 blades single rotor

4 Blades	Averaged Value
Thrust (N)	16,86
Torque (N*m)	1,33
Power (watt)	348,47
Thrust/Power	0,048

Thrust value with respect to rotor spacing of 2 blades coaxial rotor is given in figure 18. And torque value with respect to rotor spacing of 2 blades coaxial rotor is given in Figure 19.

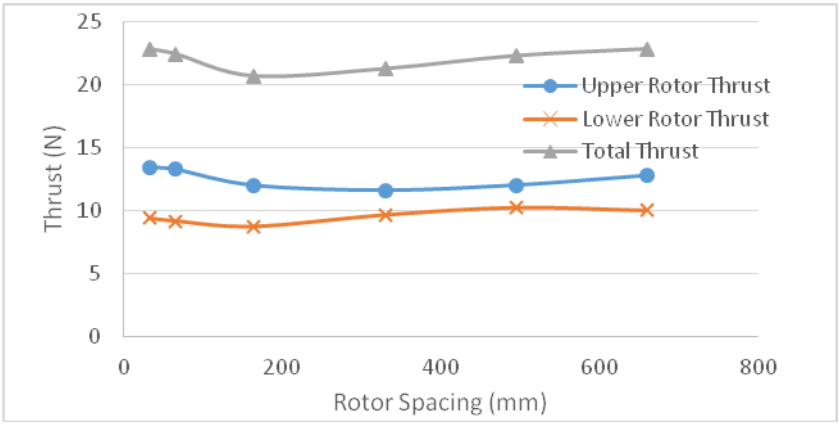

Figure 18. Thrust results of 2 blades rotor

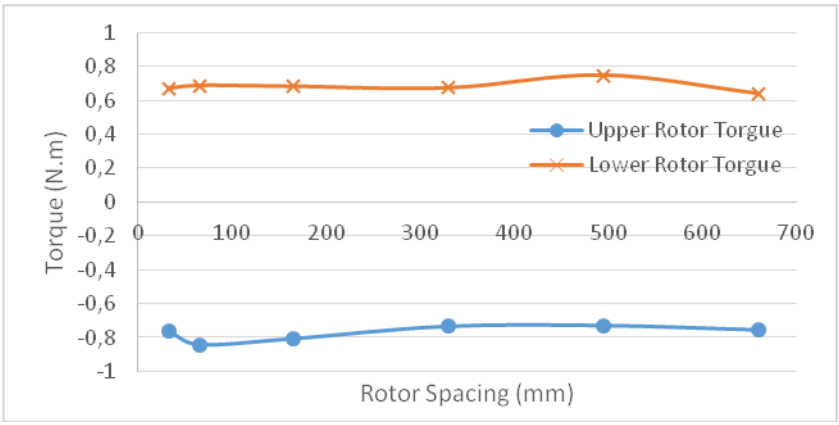

Figure 19. Torque results of 2 blades rotor

Thrust value with respect to rotor spacing of 3 blades coaxial rotor is given in Figure 20. And torque value with respect to rotor spacing of 3 blades coaxial rotor is given in Figure 21.

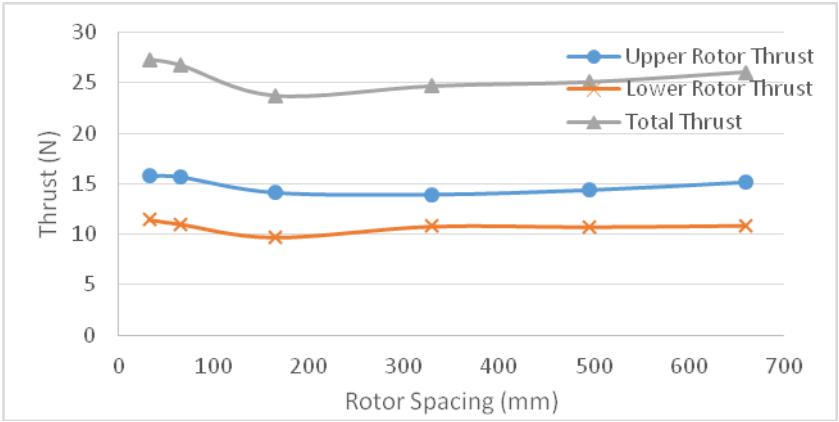

Figure 20. Thrust results of 3 blades rotor

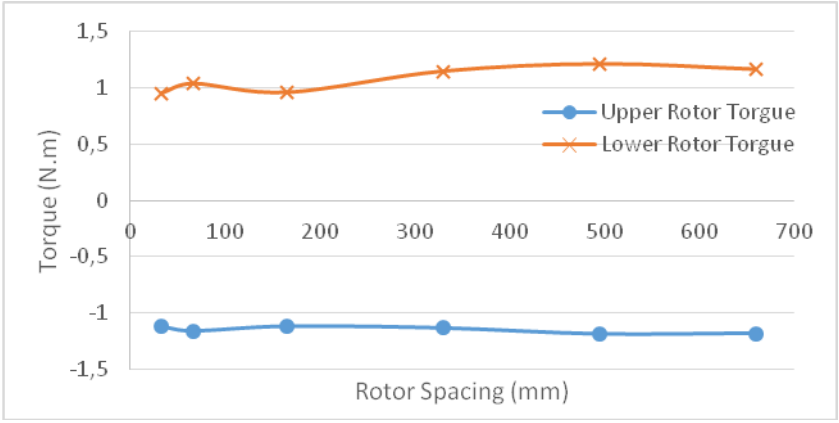

Figure 21. Torque results of 3 blades rotor

Thrust value with respect to rotor spacing of 4 blades coaxial rotor is given in Figure 22. And torque value with respect to rotor spacing of 4 blades coaxial rotor is given in Figure 23.

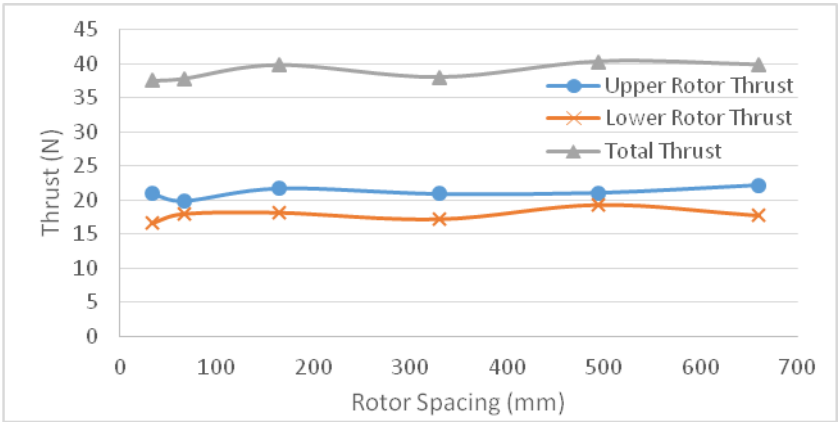

Figure 22. Thrust results of 4 blades rotor

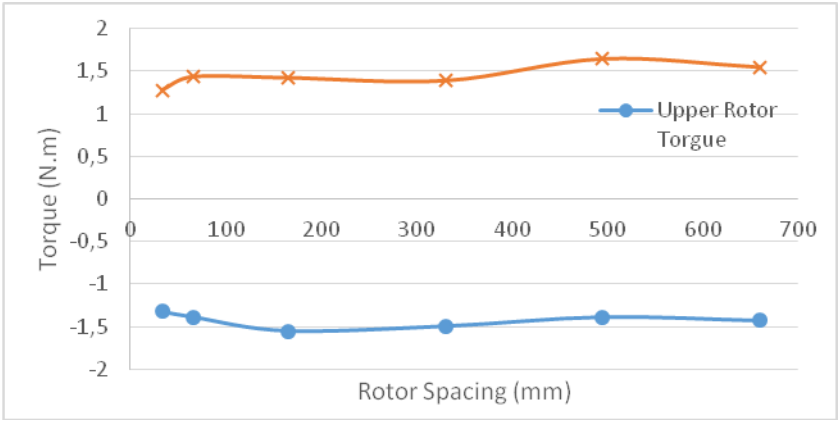

Figure 23. Torque results of 4 blades rotor

A comparison of the thrust values of the upper rotor for different blade numbers is given in Figure 24.

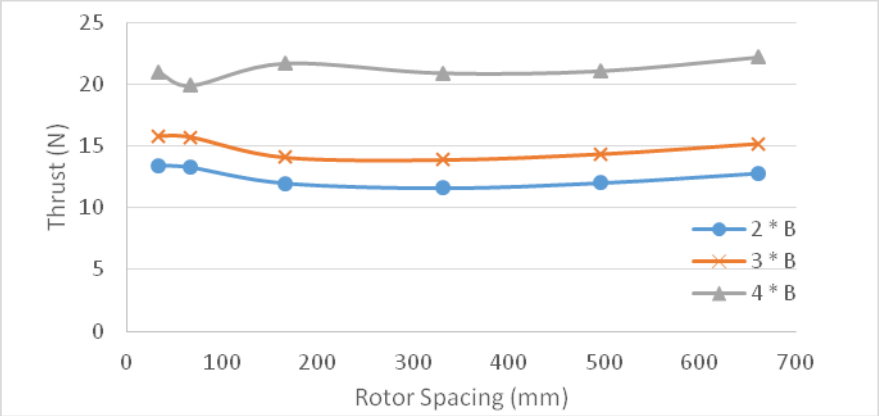

Figure 24. Thrust results of the upper rotor

A comparison of the thrust values of the lower rotor for different blade numbers is given in Figure 25.

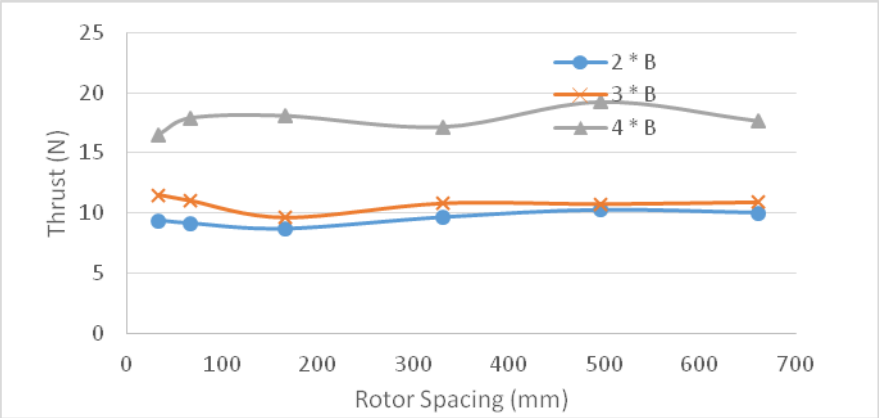

Figure 25. Thrust results of the lower rotor

A comparison of torque values of the upper rotor for different blade numbers is given in Figure 26.

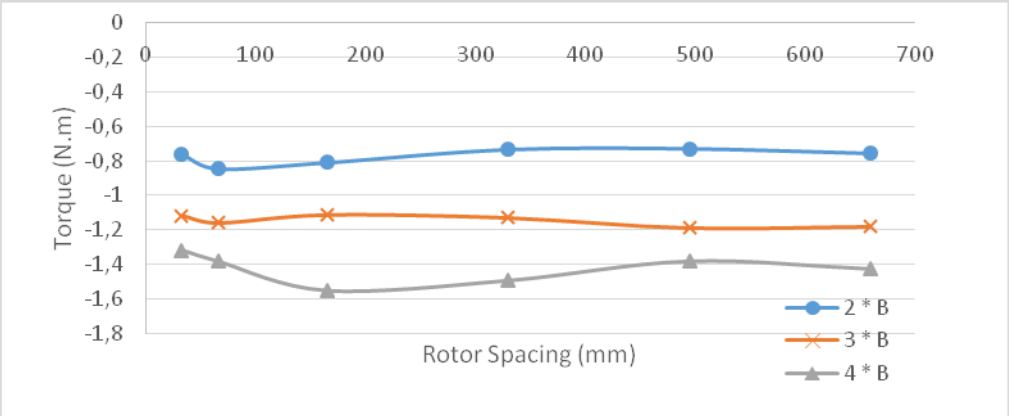

Figure 26. Torque results of the upper rotor

A comparison of torque values of the lower rotor for different blade numbers is given in Figure 27.

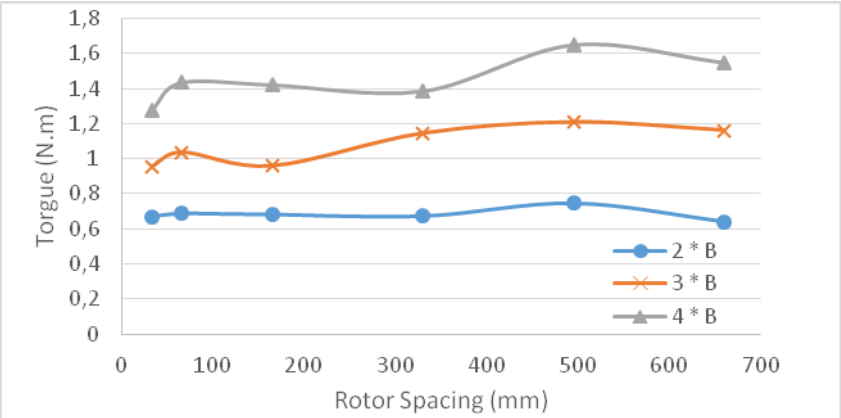

Figure 27. Torque results of the lower rotor

A comparison of the power values of the upper rotor for different blade numbers is given in Figure 28.

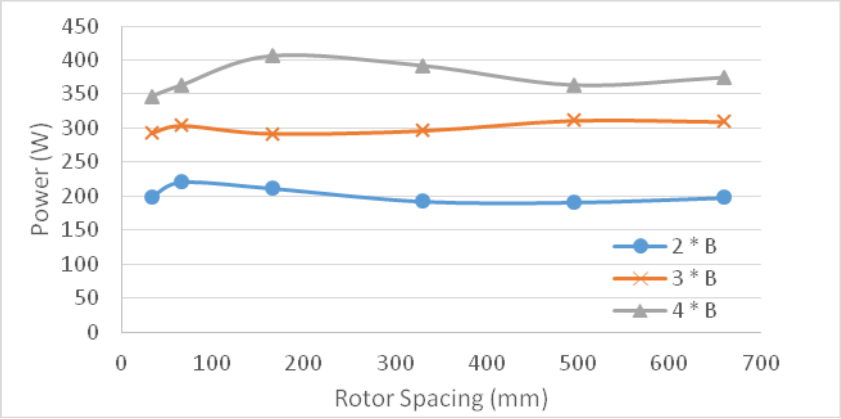

Figure 28. Power results of the upper rotor

A comparison of the power values of the lower rotor for different blade numbers is given in Figure 29.

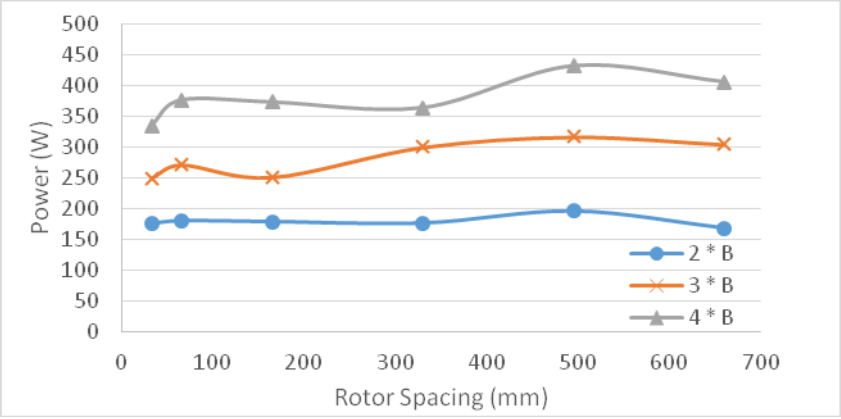

Figure 29. Power results of the lower rotor

Comparison of thrust/power ratio of the upper rotor, lower rotor and total is given in Figure 30, Figure 31 and Figure 32 respectively.

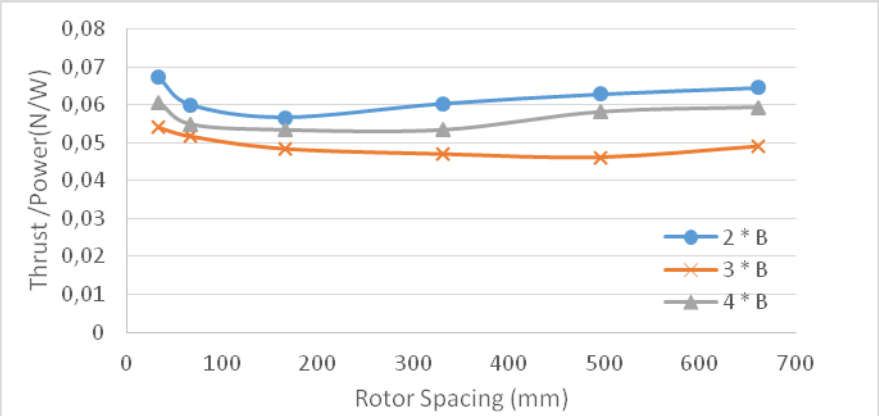

Figure 30. Thrust/Power results of the upper rotor

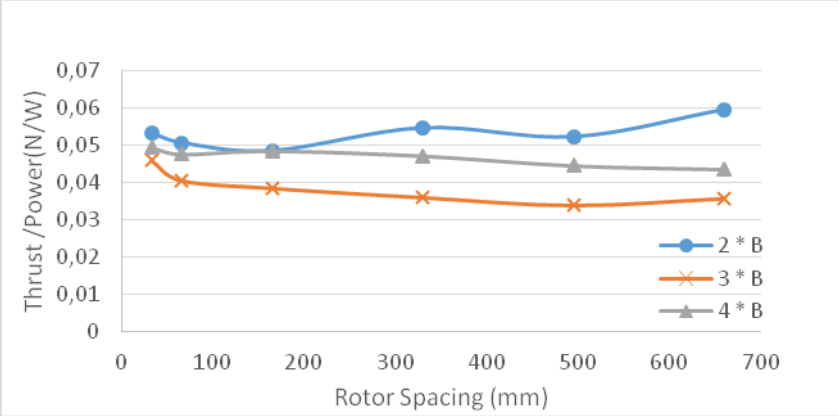

Figure 31. Thrust/Power results of the lower rotor

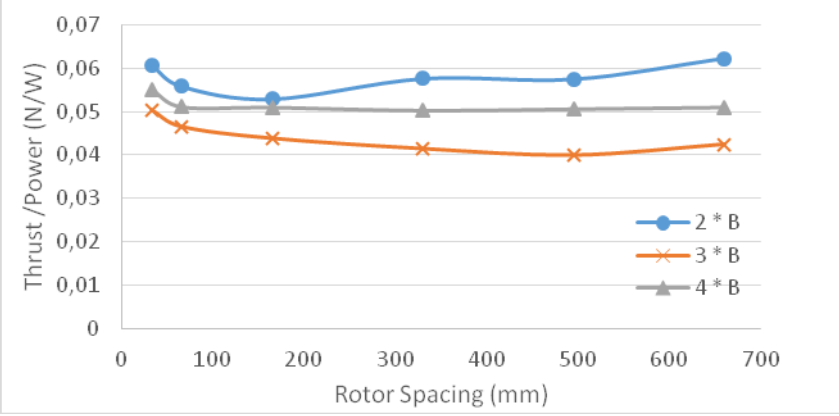

Figure 32. Total Thrust/Power results

3. Conclusions

In this study, rotor spacing and blade number of rotor concepts are investigated. Within this scope, thrust, torque and power values of the rotor, which have different blade numbers (2, 3 and 4 blades) are examined. The CFD analysis is used to perform the suggested study. The velocity and pressure distribution are obtained according to boundary and flow conditions. The maximum tip velocity is obtained by nearly 112.67 m/s for all rotors. As can be understood from the obtained speed value, the tip speed of the rotors does not exceed the speed of sound. Power value increased in proportion to the number of blades. It has been observed that the amount of increase in thrust is low in 3-blade rotor compared to the number of 2 blades, but there is more increase in 4-blade rotor compared to 2 and 3-blade rotor. It was found that the torque value in the lower rotor is higher due to the pressure difference between the lower rotor and the upper rotor. At the end of the study, it was determined that the torque value is increasing linearly with respect to the blade number. But, thrust value does not increase linearly as torque value. This means that the power requirement is increasing non-linearly due to blade number.

References

[1]. The Wikipedia website. [Online]. Available: https://en.wikipedia.org/wiki/Propeller, 2016.

[2]. Noh M. H. M.; Rashid H.; Hamid A. H. A.; Iskandar M. F, Comparison of Numerical Investigation on Airfoil and Flat Louvers on the Air Duct Intake, Procedia Engineering, 2012, 41, 1761 – 1768.

[3]. Fang-Wen H.; Shi-Tang D., Numerical Analysis for Circulation Distribution of Propeller Blade, Journal of hydrodynamics, 2010, 22(4): 488-493.

[4]. Ueno M.; Tsukada Y., Estimation of full-scale propeller torque and thrust using free-running model ship in waves, Ocean Engineering, 2016, 120, 30–39.

[5]. Driss Z.; Mlayeh O.; Driss D.; Maaloul M.; Abid M. S., Numerical simulation and experimental validation of the turbulent flow around a small incurved Savonius wind rotor, Energy, 2014, 74, 506-517.

[6]. Doğru M. H.; Güzelbey İ. H.; Göv İ., Ducted Fan Effect on the Elevation of a Concept Helicopter When the Ducted Faintail is Located in a Ground Effect Region, Journal of Aerospace Engineering, 2016, 29(1), 04015030.

[7]. Lei Y.; Bai Y.; Xu Z.; Gao Q.; Zhao C., An experimental investigation on aerodynamic performance of a coaxial rotor system with different rotor spacing and wind speed, Experimental Thermal and Fluid Science, 2013, 44, 779–785.

[8]. Göv İ., Blade Number Effect on the Thrust, Torque and Power of Propeller, International Conference on Advanced Technology & Sciences, 2016, 1435-1438.

[9]. Yoon S., Chan W. M., and Pulliam T. H., Computations of Torque-Balanced Coaxial Rotor Flows, AIAA SciTech 2017,

[10]. Hana S., Songa W., Hana Z., Lib S., Lin Y., Hybrid inverse/optimization design method for rigid coaxial rotor airfoils considering reverse flow, Aerospace Science and Technology, 2019, 95, 105488.

[11]. Kavuran G., Alagoz B. B., Ates A., Yeroglu C., Implementation of Model Reference Adaptive Controller with Fractional Order Adjustment Rules for Coaxial Rotor Control Test System Balkan Journal Of Electrical & Computer Engineering, DOI: 10.17694/bajece.93236

[12]. Shukla D. and Komerath N., Multirotor Drone Aerodynamic Interaction Investigation, Drones 2018, 2, 43; doi:10.3390/drones2040043

[13]. Feil R., Hajek M., Rauleder J., Vibratory load predictions of a high-advance-ratio coaxial rotor system validated by wind tunnel tests, Journal of Fluids and Structures, 2020, 92, 102764

[14]. Gül İ. and Kolip A., Parça Kanatlı Savonius Rüzgâr Türbin Performansının İncelenmesi, El-Cezerî Journal of Science and Engineering, 2018, 5, 3, 816-827.

[15]. Chen Y., Hu L., Liu S., Huang D., Forward/Reverse Attitude Solution and Specificity Analysis for Independent Pitch Control System of Coaxial Dual-Rotor Compound Helicopter, Arab J Sci Eng, 2018, 43, 1205–1224.

[16]. Jiang Y., Li H., Jia H., Aerodynamics Optimization of a Ducted Coaxial Rotor in Forward Flight Using Orthogonal Test Design, Shock and Vibration, 2018, doi: 10.1155/ 2018/ 2670439.

[17]. Yuan Y., Thomson D., Chen R., Propeller Control Strategy for Coaxial Compound Helicopters, Proceedings of the Institution of Mechanical Engineers Part G: Journal of Aerospace Engineering, 2018, doi:10.1177/0954410018806796

[18]. Ferguson K., Thomson D., Performance comparison between a conventional helicopter and compound helicopter configurations, Proceedings of the Institution of Mechanical Engineers, Part G: Journal of Aerospace Engineering, 2015.

[19]. Santos-Medina G., Heras-Gaytan K.Y., Martinez-Garcia E.A., Torres-Cordoba R., Carrillo-Saucedo V., Induced Force Hovering of Spherical Robot by Under-Actuated Control of Dual Rotor, book chapter 2, doi: 10.5772/63548.

[20]. Kim H.W., Kenyon A.R., Duraisamy K., Brown R.E., Interactional aerodynamics and acoustics of a hingeless coaxial helicopter with an auxiliary propeller in forward flight, 9th International Powered Lift Conference, July 2008, London, England.

[21]. Enconniere J., Ortiz-Carretero J., Pachidis V., Mission optimisation for a conceptual coaxial rotorcraft for taxi applications, Aerospace Science and Technology, 2018, 72, 14–24.

[22]. Enconniere J., Ortiz-Carretero J., Pachidis V., Mission performance analysis of a conceptual coaxial rotorcraft for air taxi applications, Aerospace Science and Technology, 2017, 69, 1–14.

[23]. Lyu W.L., Xu G.H., Interactional Effect of Propulsive Propeller Location on Counter-Rotating Coaxial Main Rotor, Journal of Aircraft, 2018, 55, 6.

[24]. The airfoiltools website. [Online]. Available: http://airfoiltools. Com /airfoil /details? airfoil= naca4415-il, 2016.